

## Magnetic Structures of SrIrO<sub>3</sub>/SrTiO<sub>3</sub> Superlattices Studied by Resonant X-Ray Diffraction

5d Ir oxides have an interplay of spin-orbit coupling and electron correlations. We investigated the magnetic structure of a SrIrO<sub>3</sub>/SrTiO<sub>3</sub> superlattice by resonant X-ray diffraction. We observed the (0.5, 0.5, 5) peak, which indicates in-plane antiferromagnetic ordering and interlayer ferromagnetic coupling. Together with the weak ferromagnetic moment in the superlattice observed only for magnetic field parallel to the IrO<sub>2</sub> plane, we concluded that in-plane canted antiferromagnetism is realized in this superlattice. These results show that we can design and realize novel electronic phases in the unit of the SrIrO<sub>3</sub> monolayer.

The novel interplay of spin-orbit coupling (SOC) and electron correlations in complex Ir oxides (iridates) has recently emerged as a new paradigm for correlated electron physics. The transition from semimetallic SrIrO<sub>3</sub> to magnetic insulator Sr<sub>2</sub>IrO<sub>4</sub> is reported in Ruddlesden-Popper series Sr<sub>n+1</sub>Ir<sub>n</sub>O<sub>3n+1</sub> ( $n = 1, 2, \text{ and } \infty$ ), suggesting a dimensionality controlled bandwidth via  $n$  [1]. Matsuno *et al.* reported transport and magnetic behaviors of synthesized artificial superlattice [(SrIrO<sub>3</sub>) <sub>$m$</sub> , SrTiO<sub>3</sub>] with  $m = 1, 2, 3, 4, \text{ and } \infty$  [2]. We tracked the evolution of electronic ground states by varying  $m$  to understand the close links among semimetal-insulator transition, magnetism, and underlying lattice structures. **Figure 1a** shows the schematics of the superlattices [(SrIrO<sub>3</sub>) <sub>$m$</sub> , SrTiO<sub>3</sub>] ( $m = 1, 2, \text{ and } \infty$ ). In this work, we investigated the magnetic structure of the SrIrO<sub>3</sub>/SrTiO<sub>3</sub> ( $m = 1$ ) superlattice by resonant X-ray diffraction to clarify the exact magnetic structure [2].

The SrIrO<sub>3</sub>/SrTiO<sub>3</sub> superlattice sample was fabricated on SrTiO<sub>3</sub>(001) substrate by a pulsed laser deposition (PLD) technique. The details of the sample fabrication were described elsewhere [2]. Resonant X-ray diffraction measurements were performed at beamline 3A at Photon Factory, KEK. Photon polarization of the  $\sigma\text{-}\pi'$  channel was selectively measured by using a Mo(400) analyzer crystal.

**Figure 1b** shows the temperature dependence of the magnetization measured at 0.1 T for the SrIrO<sub>3</sub>/SrTiO<sub>3</sub> superlattice. The weak ferromagnetic moment in the superlattice was indeed observed only for magnetic field parallel to the IrO<sub>2</sub> plane. This is consistent with the idea that weak moments originate from the Dzyaloshinskii-Moriya (DM) interaction associated with the in-plane rotation of IrO<sub>6</sub> octahedra. **Figure 1c** shows the temperature dependence of the magnetic X-ray diffraction intensity for the (0.5, 0.5, 5) peak measured at Ir  $L_3$  edge with  $\sigma\text{-}\pi'$  polarization to extract the magnetic contribution [3]. Here, the unit cell dimensions are  $a \times a \times 2a$  ( $a \sim 0.39 \text{ nm}$ ). This peak shows the in-plane antiferromagnetic ordering. From these results, we conclude

that an in-plane canted antiferromagnetism is realized in this superlattice, similar to the single layer perovskite Sr<sub>2</sub>IrO<sub>4</sub>.

Since magnetic diffraction with the integer  $c$ -axis index (0.5, 0.5, 5) was observed, the interlayer coupling of Ir local moments is ferromagnetic, in marked contrast to the bulk Sr<sub>2</sub>IrO<sub>4</sub>. This is naturally expected because the interlayer coupling of Ir moments through the hybridization with the inserted SrTiO<sub>3</sub> layer should give rise to a ferromagnetic Ir-Ir coupling regardless of whether the Ir-Ti coupling is ferromagnetic or antiferromagnetic. **Figure 1d** shows the obtained magnetic and lattice ordering pattern of this superlattice. Here, the IrO<sub>6</sub> octahedra in the two adjacent IrO<sub>2</sub> layers rotate in the same direction, which can account for ferromagnetic coupling of both canted moments and Ir moments.

The canted moment observed for the SrIrO<sub>3</sub>/SrTiO<sub>3</sub> superlattice was 0.02  $\mu_B/\text{Ir mol}$ . This is  $\sim 1/4$  of the 0.075  $\mu_B/\text{Ir mol}$  value in the bulk Sr<sub>2</sub>IrO<sub>4</sub> [4], which implies the reduction of the local Ir moment and/or the reduction of DM interaction. The in-plane lattice constant  $a \sim 0.3905 \text{ nm}$  for the superlattice sample is larger than the 0.3890 nm value for Sr<sub>2</sub>IrO<sub>4</sub> [4] and therefore a smaller rotation of the IrO<sub>6</sub> octahedra is expected for the superlattice. We estimated a rotation angle of approximately 8° in the superlattice. The Ir-O-Ir bond closer to 180° in the superlattice should decrease the strength of the DM interaction and increase the bandwidth. The latter makes the system more itinerant and reduces the magnitude of the magnetic moments. We therefore conclude that the reduced distortion of the lattice is responsible for the reduced canted moments in the superlattice.

In summary, we performed a resonant X-ray diffraction study of the SrIrO<sub>3</sub>/SrTiO<sub>3</sub> superlattice to determine the magnetic structure. We observed in-plane canted antiferromagnetism similar to the bulk Sr<sub>2</sub>IrO<sub>4</sub>, and ferromagnetic interlayer coupling in contrast to Sr<sub>2</sub>IrO<sub>4</sub>. These results show that we can design and realize novel electronic phases in the unit of the SrIrO<sub>3</sub> monolayer.

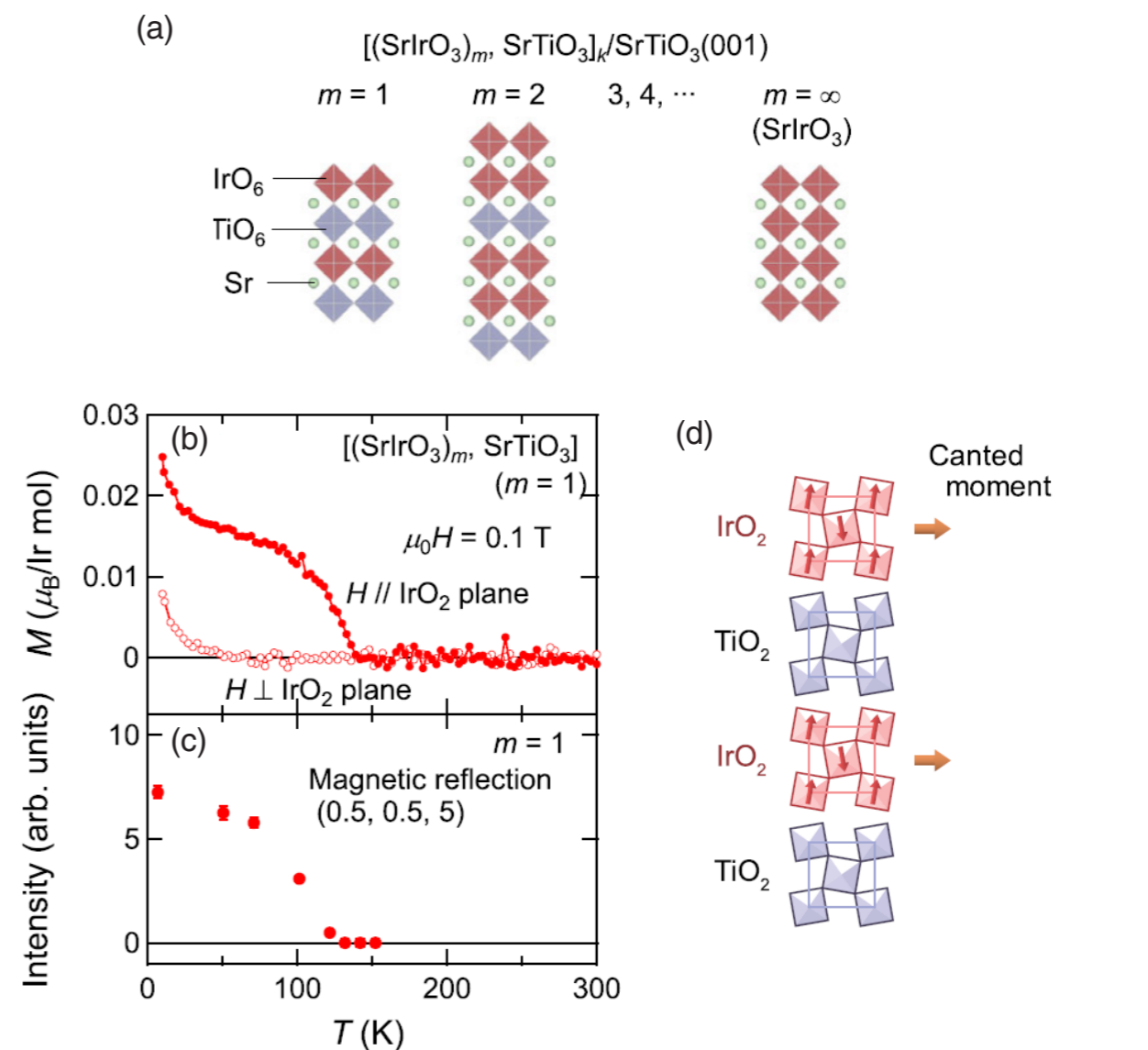


**Figure 1:** (a) Schematics of the superlattices [(SrIrO<sub>3</sub>) <sub>$m$</sub> , SrTiO<sub>3</sub>] ( $m = 1, 2, \text{ and } \infty$ ). (b) Temperature dependence of the magnetization measured at 0.1 T for the SrIrO<sub>3</sub>/SrTiO<sub>3</sub> superlattice. (c) Temperature dependence of the magnetic X-ray diffraction intensity for the (0.5, 0.5, 5) peak. (d) Magnetic structures of the SrIrO<sub>3</sub>/SrTiO<sub>3</sub> superlattice.

### REFERENCES

- [1] S. J. Moon, H. Jin, K. W. Kim, W. S. Choi, Y. S. Lee, J. Yu, G. Cao, A. Sumi, H. Funakubo, C. Bernhard and T. W. Noh, *Phys. Rev. Lett.* **101**, 226402 (2008).
- [2] J. Matsuno, K. Ihara, S. Yamamura, H. Wadati, K. Ishii, V. V. Shankar, H.-Y. Kee and H. Takagi, *Phys. Rev. Lett.* **114**, 247209 (2015).
- [3] J. P. Hannon, G. T. Trammell, M. Blume and D. Gibbs, *Phys. Rev. Lett.* **61**, 1245 (1988).
- [4] B. J. Kim, H. Ohsumi, T. Komesu, S. Sakai, T. Morita, H. Takagi and T. Arima, *Science* **323**, 1329 (2009).

### BEAMLIN

BL-3A

J. Matsuno<sup>1</sup>, K. Ihara<sup>2</sup>, S. Yamamura<sup>2</sup>, H. Wadati<sup>2</sup>, K. Ishii<sup>3</sup>, V. V. Shankar<sup>4</sup>, H.-Y. Kee<sup>4,5</sup> and H. Takagi<sup>1,2</sup> (<sup>1</sup>RIKEN, <sup>2</sup>The Univ. of Tokyo, <sup>3</sup>JAEA, <sup>4</sup>Univ. of Toronto, <sup>5</sup>CIFAR)